Article

The Development of a Superhydrophobic Surface Using Electrolytic Deposition & Polymer Chains Precipitation

Heeyun Kim*[1], Katelyn Woo*[1], MacRae Maxfield[1]

[1] Brooklyn Technical High School, Brooklyn, NY

* Equal contribution was made during this research

SUMMARY

The useful life of infrastructure metals is limited by prolonged exposure to water and deposition of insoluble minerals. Advances in surface treatment suggest that both problems can be alleviated through the formation of surfaces that are hydrophobic and therefore self-cleaning. In nature, the surface of a lotus leaf displays superhydrophobicity, containing microbumps on the surface with non-polar nanofibers on the bumps. Here, we describe a process that mimics this topography. The process includes brief electrodeposition of zinc from aqueous $Zn(NO_3)_2$ followed by drying and spray-coating of a xylene silicone solution. Our results indicate that zinc coated steel has a contact angle of 130° and a sliding angle of 16°, displaying it has high hydrophobicity and self-cleaning properties. Copper yielded similar results, indicating that this method can be applied to other metals. These results suggest that a Cassie-Baxter state, the ideal droplet to surface interaction, was formed on these metal surfaces. However, further development should be done regarding the precipitation of nanofibers to maintain the created topography. Such hydrophobic surfaces would improve the longevity of metal infrastructure since its anti-rusting characteristics limits the surface's exposure to water.

INTRODUCTION

In this era, there are many complications regarding infrastructure. This includes the maintenance of pipes and scaffolding. Within 20 years of construction, mineral deposits collect in a pipe system, preventing water flow through the pipes efficiently (1) and result in frequent cleansing or replacements of pipes. Another problem is the maintenance of scaffolding. During construction projects, scaffolding is exposed to water which leads to corrosion. However, a durable, self-cleaning surface can reduce the deposits in pipes (2) and corrosion of scaffolding (3).

Hydrophobicity is defined as the surface's chemical and physical ability to repel water. There are two measurements that quantify the surface's hydrophobicity: contact angle and sliding angle of water droplets (13). The contact angle is the angle between the tangent line of the water droplet to the surface (**Figure 1A**). The sliding angle is the angle of the surface in which the water droplet begins to roll off (**Figure 1B**) (13, 14). The higher the contact angle and the lower the sliding angle, the more hydrophobic the surface is. For example, the surface with contact angle of > 90° and sliding angle of <

45° is classified as hydrophobic, and the surface with contact angle of > 150° and sliding angle of < 10° is classified as superhydrophobic (13).

In nature, lotus leaves have superhydrophobic properties where their contact angles are greater than 150° and sliding angles are less than 5° (13). Since sliding and contact angles do not depend on each other, measuring both is needed to successfully determine the hydrophobicity of a surface.

Superhydrophobicity of a lotus leaf has been attributed to its microbumps on the surface of the leaf and the nanofibers coating the microbumps with dimensions of 10–15 μm apart, 5–10 μm in height, and 5 μm in diameter (17). These components enable the lotus leaf to achieve a Cassie-Baxter State rather than a Wenzel State (**Figure 2**). In the Cassie-Baxter State, the water droplet sits only on the tips of the bumps, creating a layer of air between the surface and the water droplet (13, 18). In the Wenzel State, the water droplet seeps through the crevices of the surface, wetting the whole surface area (16, 18).

The Cassie-Baxter state is achieved in lotus leaves not only by the size and space of the microbumps, but also by its nanofibers- the outermost fibers that create low surface energy. Surface energy is the amount of energy that attracts a liquid to its solid surface (**Figure 3**). If the attraction from
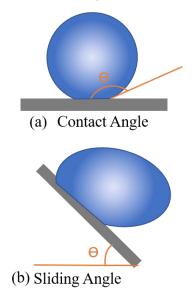

Figure 1: Illustration of water droplets (blue circle) on a surface (grey rectangle). The top orange angle represents the contact angle (the angle between the tangent line of the water droplet to the surface) and the bottom orange angle represents the sliding angle (the angle of the surface in which the water droplet begins to roll off). The higher the contact angle and lower the sliding angle, the more hydrophobic the surface is.
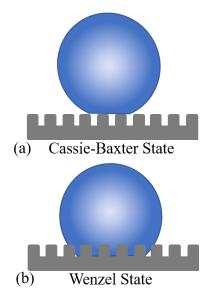
Figure 2: Diagram comparing water droplets in the Cassie-Baxter state and Wenzel state respectively. In the Cassie Baxter state, the water droplet sits on top of the microbumps, making the surface more hydrophobic than the Wenzel state where the water droplet encompases the whole surface area.

the surface to the water droplet is less than the inward force of surface tension to the water, the water droplet will tend to keep a spherical shape, creating a high contact angle. When a surface has lower surface energy, the surface is considered more hydrophobic. This is summarized in Young's Equation, which shows the relationship between surface energy, surface tension of the water, and the water's contact angle (**Figure 4**) (13, 15, 16).

We hypothesized that hydrophobicity can be imparted on industrial metal surfaces including zinc and copper by electrodeposition (**Figure 5**) and can be further enhanced through the precipitation of hydrophobic polymer chains (**Figures 6 & 7**). Due to zinc and copper's various uses in the industrial market, we examined the different electrodeposition conditions of zinc on zinc and copper on copper sheets with and without a silicone coating and evaluated the resulting metals through their contact angle and sliding angles at room temperature. From our results, electrodeposition alone achieved a contact angle of 129° and a sliding angle of 23°.
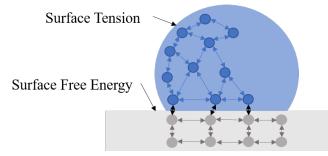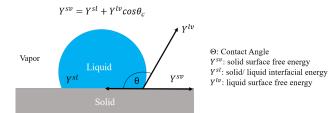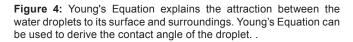

Figure 3: Illustration of intermolecular forces of a water droplet to its surface. Water molecules (dark blue circles) are held together through hydrogen bonding, creating surface tension. When surface tension is much greater than surface free energy, the water molecule displays a round shape that makes the surface hydrophobic. Surface free energy provides a quantitative measure to the intermolecular strength.
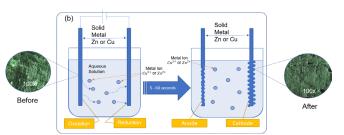

$$Y^{sv} = Y^{sl} + Y^{lv}cos\theta_c$$

Θ: Contact Angle
Y^{sv}: solid surface free energy
Y^{sl}: solid/ liquid interfacial energy
Y^{lv}: liquid surface free energy

Figure 4: Young's Equation explains the attraction between the water droplets to its surface and surroundings. Young's Equation can be used to derive the contact angle of the droplet. .

Figure 5: Illustration of electroplated microparticles (zinc or copper) on a metal surface (zinc or copper). For zinc surfaces, $Zn(NO_3)_2$(aq) was used to develop the zinc microbumps on the zinc surface. Likewise, $CuSO_4$(aq) was used to develop the microbumps on copper surfaces. Each surface was plated for a given time period between 5 and 60 seconds. This illustration depicts the before and after of a zinc plated surface under a microscope to present the created microbumps.

The sliding angle was further enhanced by the silicone coating which reached 15°. Since the hydrophobicity of zinc and copper was improved by this treatment, we concluded that this method could be applied in industry such as developing anti-corroding bridges, pipes, and scaffolding.
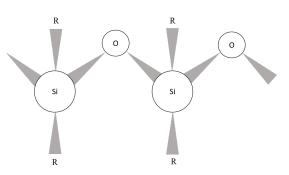

Figure 6: Illustration of the atomic structure of silicone. In this experiment, silicone was used to mimic the nanofiber hairs of the lotus leaf. In this structure, the repeating R groups of silicone makes it an ideal polymer chain for hydrophobic surfaces.
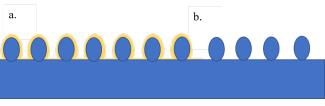

Figure 7: Illustration of a before and after image of silicone sprayed on a microbump surface. A thin layer of silicone is ideal for this surface as too much silicone will heavily cover the created microbumps.

Time (s)	Contact Angles for Droplets (°)					Average (°)	Standard Dev
	1	2	3	4	5		
Control:	71	52	68	67	63	64	7.4
5	110	115	104	123	106	112	6.8
10	118	115	125	128	119	121	4.8
15	119	113	107	123	97	112	9.1
20	125	112	104	131	117	118	9.6
25	115	116	131	117	128	121	6.9
30	125	118	121	118	121	120	2.3
35	115	112	123	125	124	120	5.5
40	130	121	128	136	131	129	5.1
45	139	134	134	127	113	129	8.8
50	130	130	121	126	129	127	3.3
55	118	101	103	102	102	105	6.5
60	113	95	93	101	91	99	8.0

Table 1: Zinc Contact Angle over Plating Time without Silicone Layer.

Time(s)	Contact Angle for Droplets (°)					Average (°)	Standard Dev
	1	2	3	4	5		
Control:	125	111	95	94	102	106	13.1
5	125	123	113	121	118	120	4.4
10	133	132	139	118	130	130	6.9
15	97	105	101	96	91	98	4.9
20	119	129	113	125	120	121	5.4
25	132	127	120	116	117	122	6.1
30	129	121	128	122	110	122	6.6
35	121	129	103	117	117	117	8.4
40	132	117	119	140	123	126	8.5
45	123	123	133	128	144	130	7.8
50	133	126	113	109	135	123	10.5
55	127	121	134	124	113	124	6.8
60	138	127	100	133	119	132	13.4

Table 2: Zince Contact Angle over Plating Time after Spraying Silicone Layer.

RESULTS

In this experiment, we cleaned flat metal sheets (zinc and copper), which then underwent an electrodeposition treatment. After drying, the surface was sprayed with a silicone layer to enhance its hydrophobicity. Contact angle and sliding angle were recorded in five second intervals. The size of the metal sheet, amount of silicone sprayed on the sheet, and the concentrations of the aqueous solutions ($CuSO_4$ and $Zn(NO_3)_2$) used for the electrodeposition process were kept constant.

Contact angles

Here, zinc contact angles were collected and examined to determine the effectiveness of electroplating methods in surface hydrophobicity. Over time, the contact angle generally increased until it peaked at 45 s. After, the contact angles began to decrease.

After creating microbumps with electrodeposition, a layer of silicone was sprayed to mimic the long chains of hydrocarbons on a lotus leaf. From the data, the contact angles with silicone generally stayed within the same range of values.

In order to examine the extent of the electrodeposition method, we also applied this method to copper. The contact angle increased until 15 s then showed slight decrease after its optimal time.
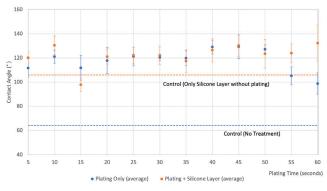
The contact angle of zinc with electroplating treatment only peaked at 45 s (**Figure 8, Tables 1 & 2**). Both plating with and without silicone generally followed a similar trend, where plating with silicone slightly enhanced the contact angle. As a result, electroplating microbumps greatly enhanced the hydrophobicity of the metal surface compared to the surface with only the silicone layer and control. However, the hydrophobicity before 45 s was not enhanced by the silicone possibly because the hydrophobicity from silicone was negligible compared to the hydrophobicity from the microbumps.

The general trend of zinc (increase in the beginning and decrease after peak) was also present in copper (**Figure 9, Table 3**). Therefore, electroplating methods can be applied to different metals. However, since the peak of copper is at 15 s instead of 45 s, different metals can have different optimal plating times. Copper most likely had an earlier peak because it is a more noble metal.

Sliding angles

The sliding angles of water droplets also were collected and examined to study the surface's hydrophobicity in terms of sliding angle. When zinc was treated with only electrodeposition, the sliding angles showed rapid decrease in the beginning and plateaued after 25 s.

When the electrodeposited surfaces were coated with a silicone layer, there was a significant decrease in sliding angle compared to the non-silicone coated surface. Additionally, there was a general decrease in sliding angle over the electroplating time.
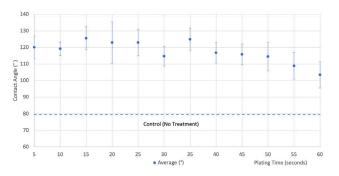

Figure 8: Zinc Contact Angle vs. Time of plating. A zinc surface was electroplated for different lengths of time (5–60 s) and the resulting contact angle was measured for each time point, with and without a silicone layer. Measurements were taken for four conditions: no treatment control (blue dashed line), silicone control (orange dashed line), electroplated only (blue), and electroplated with a silicone layer (orange) (n = 5 for each condition). Error bars represent one standard deviation.

Figure 9: Copper Contact Angles without Silicone. A copper surface was electroplated for a different range of time (5-60 s), and the contact angle measurements were taken in a 5 s interval. The control (contact angle of the non-treated copper surface) is also shown in dotted line (n=5 for both control and treated surface). The error bars represent one standard deviation.

	Contact Angle for Droplets (°)						
Time (s)	1	2	3	4	5	Average (°)	Standard Dev
Control:	91	77	83	75	72	80	7.6
5	114	116	122	129	--	120	5.3
10	114	117	119	124	122	119	3.2
15	136	127	119	127	119	126	5.6
20	130	135	128	103	119	123	10.2
25	127	135	117	119	117	123	6.4
30	119	112	123	111	109	115	4.8
35	128	127	133	115	122	125	5.5
40	115	118	118	107	125	117	5.1
45	112	107	121	119	120	116	5.1
50	117	112	101	120	123	114	7.0
55	115	100	105	104	119	109	6.5
60	104	117	98	100	98	103	6.5

Table 3: The Contact Angle over Electroplating Time of Copper Surface without Silicone Layer.

	Contact Angle for Droplets (°)						
Time (s)	1	2	3	4	5	Average (°)	Standard Dev
Control:	13	15	12	11	11	12	1.5
5	14	13	20	16	16	16	2.2
10	21	14	23	19	20	19	3.1
15	17	14	17	15	16	16	1.0
20	17	17	13	24	21	18	3.6
25	17	14	16	13	15	15	1.5
30	15	13	14	13	22	15	3.5
35	13	14	11	15	14	13	1.4
40	10	16	19	15	12	14	3.1
45	13	19	20	13	20	17	3.2
50	15	20	19	22	15	18	2.9
55	12	12	16	16	12	13	2.0
60	17	13	14	16	15	15	1.4

Table 5: Sliding Angle over Electroplating Time of Zinc Plated Surfaace with Addition of Silicone Layer.

As plating time increased, the sliding angle without a silicone layer decreased, supporting the hypothesis that the electroplating method enhances hydrophobicity (**Figure 10, Table 4 & 5**). The addition of silicone also enhanced the hydrophobicity and slipperiness of the zinc surface due to the polar repulsion of the silicone. After 25 s of the plated surface without silicone, the surface reached its optimal sliding angle.

DISCUSSION

The data supported the hypothesis that when microbumps are electrodeposited on a metal surface, the surface will develop hydrophobic properties which can be further enhanced by chemical surface treatment. Electrodeposition alone could achieve a contact angle of 129° and a sliding angle of 23°. The sliding angle was further enhanced by the silicone coating to reach 15°.

The electroplating treatment enhances a surface's hydrophobicity comparing the contact angles of the treated surface and that of the control (**Figure 8**). When comparing the values between 5 and 50 s, we concluded that there were no significant changes between each individual 5 s interval. At 55 and 60 s, the contact angles were significantly lower than the preceding contact angles. As a result, electroplating time should be shorter than 55 s to produce better hydrophobicity. Additionally, there is no significant enhancement in hydrophobicity with an addition of a silicone layer. The aid of a silicone layer did not enhance the contact angle since electrodeposition itself had already produced the desired hydrophobicity.

In order to test the electroplating method on different metals, electroplating treatment was performed on copper (**Figure 9**). Comparing the control to the plated surfaces, we concluded that plating also enhances a surface's hydrophobicity on copper surfaces. However, the contact angles between each

	Contact Angle for Droplets (°)						
Time (s)	1	2	3	4	5	Average (°)	Standard Dev
Control:	10	14	15	13	10	12	2.3
5	38	42	41	39	39	40	1.7
10	36	42	29	35	--	36	4.6
15	31	26	36	39	28	32	4.9
20	18	36	37	19	37	29	9.0
25	21	21	23	16	21	20	2.3
30	25	16	27	34	27	26	5.6
35	29	21	18	21	15	21	4.6
40	25	26	23	26	26	25	1.0
45	22	21	28	20	22	23	2.8
50	19	26	25	25	28	25	3.0
55	17	17	23	21	21	20	2.6
60	23	25	21	32	24	25	3.9

Table 4: Sliding Angle of Zinc Surface without Silicone Layer over Plating Time.

interval was not significant. Yet, when comparing the change in hydrophobicity between a larger interval (ex. comparing the contact angles at 5 and 60 s), we concluded that there may be a significant change since the range of values do not overlap. Due to the significant difference between these two endpoints, the data shows that shorter electroplating time (5 s) results in better hydrophobicity than a longer electroplating time (60 s).

It was concluded that the plated surface with a silicone layer significantly enhances the surface's hydrophobicity compared to the plated surface without a silicone layer (**Figure 10**). Looking at the 'plating only' data (blue), there was a significant decrease from 5 s to 25 s with no value overlap, showing that hydrophobicity increased significantly during this time period. However, after 25 s, there were no significant changes between each 5 s interval since the values from points 25 to 60 s overlap each other. When comparing the two controls' sliding angles to the two treated surfaces' (with and without silicone) sliding angles, the controls' sliding angle proved to be lower. Additionally, when comparing the 'no treatment' control to the 'only silicone layer' control, the 'no treatment' control was also lower. As a result, the electroplated metals with and without a silicone layer and the 'only silicone layer' controlled surfaces did not contribute to the hydrophobicity of the metal surface in terms of sliding angle. Even though the data showed that hydrophobicity was
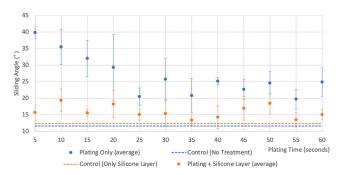

Figure 10: Zinc Sliding Angle vs. Time of Plating. Two groups of zinc surface were electroplated for different lengths of time (5-60 s), and one group of the electroplated sample was coated with a silicone layer after the electrodeposition while another was only electroplated. Measurements were taken for both groups: electroplated with a silicon layer (orange) and electroplated only (blue). The control for both groups is also shown: no treatment control (blue dashed line) and only silicon layer without electrodeposition (orange dashed line) (n = 5 for all four data). Error bars draw the range of one standard deviation.

not improved, we observed that with a silicone coating, there was no water residue left on the surface whereas surfaces without silicone, water residue was present.

For future experimentation regarding electrodeposition, optimal electrodeposition conditions (electrode geometry, current density, electrolyte composite, and temperature) that create uniform hydrophobicity across the metal surface should be collected along with applying microscopy to reveal geometry and dimensions of surface features. For copper metal surfaces, a larger range of electroplating time is needed to determine the optimal plating time. For experiments regarding the silicone coating, different dilutions, solvents, and siloxanes should be experimented with to obtain an optimal polymer coating. Additionally, different industrial metals such as aluminum and steel should be tested so that a program could be developed to predict the optimal plating time for different industrial metals.

Generally, the hydrophobicity increased in terms of contact angle, but the hydrophobicity did not improve in terms of sliding angle. Therefore, depending on the application of the hydrophobic surface, certain methods (electrodeposition, silicone layer, or both) to obtain a hydrophobic surface should be considered.

METHODS

A metal sheet (copper and zinc) was cut into 7.5 cm x 3 cm portions for manageability. All the metal portions were cleaned with acetone and dishwashing soap before experimentation in order to remove contaminants. Using two of the same types of metal strips at a time, one strip was used as an anode while the other strip was used as the cathode. The anode strip was labeled and was attached to the positive end of the battery with an alligator clip. Likewise, the cathode zinc strip was attached to the negative end of the battery using another alligator clip. Once attached to the battery, both metal portions were placed in an aqueous solution containing the metal compound for a given amount of time (**Figure 5**). The aqueous solution used for copper was with a concentration of 84 mM, and the aqueous solution for zinc was $Zn(NO_3)_2$ with a concentration of 106 mM. The rest of the materials and the times were kept constant.

After plating, the cathode strip, where microbumps have been plated by reduction, was placed in the oven (135°C) for about 15 minutes until dry. Then, it was air-dried overnight to remove any remaining liquid. Since electrodeposition is a rapid reaction, the surfaces underwent treatment in 5 s intervals to examine the surface changes in detail. This process was repeated from 5 to 60 s for each metal surface.

In addition to modifying the physical structure of the hydrophobic surface, chemical treatment was also done. Inspired from the nanofibers found on the surface of lotus plants, a polymer chain was deposited on the bumpy surface to decrease the sliding angle. Since silicone can bind with repeating R-groups to form long chains (**Figure 6**), it was used as the polymer for this experiment. Liquid silicone (product from GE Sealants & Adhesives) was dissolved into xylene in a 1:3 g ratio to reduce the silicone's viscosity. This was then sprayed onto the plated surface (**Figure 7**). As the xylene evaporated, the silicone was left behind as a precipitate, forming a layer of silicone chains.

The contact angles for all samples were measured using the ImageJ image analysis program (19). The water droplet was photographed at eye level to get an accurate contact angle. The average and standard deviation was calculated to determine an accurate representation of the data. In order to compare the effectiveness of these methods, the contact angle and sliding angle of zinc and copper without any treatment were measured. Additionally, the contact and sliding angles of zinc surfaces with only a silicone coating were measured. These controls were used as the standard of comparison between the effectiveness of the developed electroplating method and the existing method of spraying hydrophobic chemicals to the surface to create water-repellent surfaces.

REFERENCES

1. Li, Zongchen, *et al*. "External Surface Cracked Offshore Steel Pipes Reinforced with Composite Repair System Subjected to Cyclic Bending: An Experimental Investigation." *Theoretical and Applied Fracture Mechanics*, vol. 109, 2020, doi:10.1016/j.tafmec.2020.102703.
2. Shirtcliffe, Neil J., *et al*. "Superhydrophobic Copper Tubes with Possible Flow Enhancement and Drag Reduction." *ACS Applied Materials & Interfaces*, vol. 1, no. 6, 2009, pp. 1316–23. doi:10.1021/am9001937.
3. Eseev, Marat, *et al*. "Creation of Superhydrophobic Coatings Based on MWCNTs Xerogel." *Nanomaterials*, vol. 9, no. 11, 2019. doi:10.3390/nano9111584.
4. Sharma, Vipin Kumar, *et al*. "Parametric Study of Aluminium-Rare Earth Based Composites with Improved Hydrophobicity Using Response Surface Method." *Journal of Materials Research and Technology*, vol. 9, no. 3, 2020, pp. 4919–32. doi:10.1016/j.jmrt.2020.03.011.
5. Ding, Yi, *et al*. "Critical Sliding Angle of Water Droplet on Parallel Hydrophobic Grooved Surface." *Colloids and Surfaces A: Physicochemical and Engineering Aspects*, vol. 585, 2020, doi:10.1016/j.colsurfa.2019.124083.
6. Montes Ruiz-Cabello, *et al*. "Fabrication of Superhydrophobic Metal Surfaces for Anti-Icing Applications." *Journal of Visualized Experiments: JoVE*, no. 138, 2018. doi:10.3791/57635.
7. Chen, Huaxin, *et al*. "Review of Ice-Pavement Adhesion Study and Development of Hydrophobic Surface in Pavement Deicing." *Journal of Traffic and Transportation Engineering (English Edition)*, vol. 5, no. 3, 2018, pp. 224–38. doi:10.1016/j.jtte.2018.03.002.
8. V. Oriani, Andrea, *et al*. "Aluminium Electrodeposition from a Novel Hydrophobic Ionic Liquid Tetramethyl Guanidinium-Perfluoro-3-Oxa-4,5 Dichloro-Pentan-Sulphonate." *Journal of Electroanalytical Chemistry*, vol. 793, 2017, pp. 85–92. doi:10.1016/j.jelechem.2016.09.041.

9. Dalvi, Vishwanath H., and Peter J. Rossky. "Molecular Origins of Fluorocarbon Hydrophobicity." *Proceedings of the National Academy of Sciences of the United States of America*, vol. 107, no. 31, 2010, pp. 13603–07. doi:10.1073/pnas.0915169107.

10. Kwon, Min Ho, *et al*. "Fabrication of a Super-Hydrophobic Surface on Metal Using Laser Ablation and Electrodeposition." *Applied Surface Science*, vol. 288, 2014, pp. 222–28. doi:10.1016/j.apsusc.2013.10.011.

11. Wang, Daheng, *et al*. "Tomato-Lotus Inspired Edible Superhydrophobic Artificial Lotus Leaf." *Chemical Engineering Journal*, vol. 400, 2020, doi:10.1016/j.cej.2020.125883.

12. Kim, Woochan, *et al*. "Engineering Lotus Leaf-Inspired Micro- and Nanostructures for the Manipulation of Functional Engineering Platforms." *Journal of Industrial and Engineering Chemistry*, vol. 61, 2018, pp. 39–52. doi:10.1016/j.jiec.2017.11.045.

13. Ghaffari, Sepehr, *et al*. "Review of Superoleophobic Surfaces: Evaluation, Fabrication Methods, and Industrial Applications." *Surfaces and Interfaces*, vol. 17, 2019, doi:10.1016/j.surfin.2019.100340.

14. Wae AbdulKadir, Wan Aisyah Fadilah, *et al*. "Biomimetic Hydrophobic Membrane: A Review of Anti-Wetting Properties as a Potential Factor in Membrane Development for Membrane Distillation (MD)." *Journal of Industrial and Engineering Chemistry*, 2020. doi:10.1016/j.jiec.2020.08.005.

15. Shaoxian, Bai, and Wen Shizhu. "Chapter 7 - Vapor-Condensed Gas Lubrication of Face Seals." *Gas Thermohydrodynamic Lubrication and Seals*, 2019, pp. 143–65. doi:10.1016/B978-0-12-816716-8.00007-3.

16. Dai, Xianming, *et al*. "Slippery Wenzel State." *ACS Nano*, vol. 9, no. 9, 2015, pp. 9260–67. doi:10.1021/acsnano.5b04151.

17. Burton, Zachary, and Bharat Bhushan. "Surface Characterization and Adhesion and Friction Properties of Hydrophobic Leaf Surfaces." *Ultramicroscopy*, vol. 106, no. 8, 2006, pp. 709–19. doi:10.1016/j.ultramic.2005.10.007.

18. Giacomello, Alberto, *et al*. "Cassie–Baxter and Wenzel States on a Nanostructured Surface: Phase Diagram, Metastabilities, and Transition Mechanism by Atomistic Free Energy Calculations." *Langmuir*, vol. 28, no. 29, American Chemical Society, 2012, pp. 10764–72. doi:10.1021/la3018453.

19. Schneider, Caroline, *et al*. "NIH Image to ImageJ: 25 years of image analysis", *Nature Methods*, vol. 9, no. 7, 2012, pp. 671-675, doi: 10.1038/nmeth.2089.